A novel ligand with -NH_2 and -COOH-decorated Co/Fe-based oxide for efficient overall water splitting: dual modulation roles of active sites and local electronic structure

Yalan Zhang[a], *Zebin Yu*[*,a], *Ronghua Jiang*[b], *Jung Huang*[c], *Yanping Hou*[a], *Fei Yang*[d], *Boge Zhang*[a], *Yiyi Huang*[a], *Bo Ye*[a], *Runzhi Zhang*[a]

[a] School of Resources, Environment and Materials, Guangxi University, Nanning 530004, P. R. China

[b] School of Chemical and Environmental Engineering, Shaoguan University, Shaoguan 512005, P. R. China

[c] College of Civil Engineering and Architecture, Guangxi University, Nanning 530004, P. R. China

[d] Guangzhou Institution Energy Testing, Guangzhou 510170, Guangzhou, P. R. China

* Corresponding author. Tel./fax.: + 8613877108420

E-mail: xxzx7514@hotmail.com (Z. Yu)

Experimental section

1. Synthesis of (MOF(Co/Fe/COOH)) electrode

Synthesis of MOF(Co/Fe/COOH) on NF. 400 mg of terephthalic acid was dissolved in 40 mL DMF and the resulting solution was transferred into a 50 mL Teflon-lined stainless-steel autoclave. The CoFe NWs on the NF were submersed into the above solution, heated at 160 ℃ for 12 h in an electric oven and then cooled down to room temperature naturally.

2. Synthesis of Co-MOF electrode

Synthesis of precursor on NF. The commercial NF was successively cleaned with ethanol, acetone, and ethanol for 30 min each. The growth solution was prepared by dissolving 0.06 mol·L^{-1} Cobalt (II) nitrate hexahydrate and 0.25 mol·L^{-1} urea in 40 mL of deionized water. One piece of NF (1 × 3 cm) was submersed in the above solution and $Co_{0.6}$ oxide was directly grown onto the commercial NF at 100 ℃ for 3 h in an electric oven. The resulting $Co_{0.6}$ oxide was washed with ethanol twice and dried in a vacuum oven at 50 ℃ overnight.

Synthesis of Co-MOF on NF. 400 mg of 2-Aminoterephthalic Acid was dissolved in 40 mL DMF and the resulting solution was transferred into a 50 mL Teflon-lined stainless-steel autoclave. The $Co_{0.6}$ oxide on the NF was submersed into the above solution, heated at 160 ℃ for 12 h in an electric oven and then cooled down to room temperature naturally.

3. Synthesis of Fe-MOF electrode

Synthesis of precursor on NF. The commercial NF was successively cleaned with ethanol, acetone, and ethanol for 30 min each. The growth solution was prepared by dissolving 0.03 mol·L^{-1} Iron (III) nitrate nonahydrate, and 0.25 mol·L^{-1} urea in 40 mL of deionized water. One piece of NF (1 × 3 cm) was submersed in the above solution, and Fe oxide was directly grown onto the commercial NF at 100 ℃ for 3 h in an electric oven. The resulting Fe oxide was washed with ethanol twice and dried in a vacuum oven at 50 ℃ overnight.

Synthesis of Fe-MOF on NF. 400 mg of 2-Aminoterephthalic Acid was dissolved in 40 mL DMF and the resulting solution was transferred into a 50 mL Teflon-lined stainless-steel autoclave. The Fe oxide on the NF was submersed into the above solution, heated at 160 ℃ for 12 h in an electric oven and then cooled down to room temperature naturally.

4. Synthesis of Pt/C//RuO_2 electrode

Pt/C and RuO_2 catalysts were fabricated by methods elaborated elsewhere. In brief, 10 mg of 20% Pt/C or RuO_2 was dissolved in a 2 mL solution of 0.8 mL of deionized water, 1.08 mL of anhydrous ethanol and 0.12 mL of 5% Nafion solution. That mixture was then ultrasonicated for 30 min to form a homogeneous catalyst ink. Subsequently, 0.05 mL of the ink was loaded onto the NF 20 times using rotating deposition. Lastly, the sample was placed in an oven and dried for further testing.

5. Characterizations and electrochemical measurements

X-ray diffraction (XRD) was conducted to analyze the crystalline phases of the samples, which was detected by a high power polycrystalline X-ray diffractometer

(DX-2700AX) at a scanning speed of 10 ^{o} min^{-1} over degree of 5-85 ^{o}. The transmission electron microscopy (TEM, Titan G_2 ETEM) was carried out to characterize the inner structures of the catalysts. X-ray photoelectron spectroscopy (XPS) spectra was performed to gain insight into the chemical composition and binding states of the electrodes on an ESCALAB 250XI (USA) instrument with a monochromatic Al Kα X-ray source. The electrodes surface morphologies were characterized by the field-emission scanning electron microscopy (FESEM, Hitachi SU8220) and the element compositions of the electrodes were investigated by energy-dispersive X-ray spectroscopy (EDS). Fourier transform infrared (FTIR) spectroscopy was performed using a Carry 660- FT/IR in attenuated total reflection mode (resolution= 0.07 cm^{-1}). Atomic force microscopy (AFM) measurement was conducted on a Bruker edge. To test different vibrational modes of the sample, Raman spectroscopy characterization was carried out using a Leica DM 2700 microscope with an excitation wavelength of 532 nm. Resistivity testing was performed by a high precision resistivity tester (YAOS) with Four-probe method. Inductively coupled plasma atomic emission spectroscopy (ICP-AES, CAMT 2000 Thrmo Fisher Scientific) was used to determine Co and Fe loading amount on the electrodes.

All electrochemical measurements were conducted using the electrochemical workstation (CHI 660EZ, China) with a typical three-electrode system, in which with the σ-Fe/Co-N-ligand(COOH) or contrast material as the working electrode, a platinum gauze electrode as the counter electrode, a Hg| HgO | OH^- electrode as the reference, and 1 mol·L^{-1} KOH as the electrolyte. Before electrochemical tests, the

electrolyte was purged with N_2 for 30 min to remove O_2. All the potentials in our work were calculated relative to RHE, according to the Nernst equation:

$$E\ (RHE) = E\ (vs.\ Hg|\ HgO\ |\ OH^-) + 0.059\times pH + 0.098V = E\ (vs.\ Hg\ |\ HgO\ |\ OH^-) + 0.924V. \quad (1)$$

Linear sweep voltammetry (LSV) polarization curves for OER and HER were conducted with a scan rate of 1 mV s^{-1} and 5 mV s^{-1} with 95% IR compensation. Long-term durability was tested at the current density of 70 mA cm^{-2} or 50 mA cm^{-2} for 100 h by chronopotentiometry (V-t curve). Long-term test of HER and OER was determined by chronoamperometry (it) for 2 h, respectively. Electrochemical impedance spectroscopy (EIS) test was performed within the frequency range of 100 kHz~1 Hz with AC potential amplitude of 5 mV. The electrical double-layer specific capacitances (C_{dl}) of the electrodes were characterized by conducting cyclic voltammogram (CV) with various scan rates of 40, 60, 80, 100, 120 and 140 mV s^{-1} at non-Faradaic region within the potential range from 0.54 V to 0.67 V (vs. RHE).

The electrochemically active surface areas (ECSA) was determined by CV at the potential window 0.54 V to 0.67 V (vs. RHE) with different scanning rate of 40, 60, 80, 100, 120 and 140 mV s^{-1}. By plotting the difference between the anodic and cathodic current densities ($\Delta j = j_a - j_c$) at 0.609 V (vs. RHE) against the scan rates, the resulting linear slope is twice of the double layer capacitance (C_{dl}), which can be used to represent ECSA. The specific capacitance can be converted into the ECSA using the specific capacitance value for a flat standard electrode with 1 cm^2 of real surface

area (C_s), and C_s is generally in the range of 20 to 60 μF cm^{-2}. Here we use the average value of 40 μF cm^{-2} per cm_{ECSA}^2 to calculate the ECSA (Equation 2).

$$ECSA=C_{dl}/C_s \qquad (2)$$

Mass activity (j_m, A g^{-1}) is evaluated at an overpotential of η=300 mV. The mass activity is calculated from the catalyst loading m (0.32 mg cm_{geo}^{-2}) and the measured current density j_{geo} (mA cm_{geo}^{-2}) (Equation 3):

$$j_m= j_{geo}/m \qquad (3)$$

Specific activity (js, μA cm_{ECSA}^{-2}) is evaluated at an overpotential of η=300 mV. The specific activity measured current density js (μA cm_{ECSA}^{-2}) (Equation 4):

$$js=1000j_{geo}S/ECSA \qquad (4)$$

Details concerning the calculation of TOF are shown as below. The values of TOF are calculated assuming that all Co and Ni ions in the catalysts are active and contribute to the catalytic reaction (the lowest TOF values were calculated)

$$TOF = jS/(4Fn) \qquad (5)$$

Here, j (A/cm^2) is the measured current density at an overpotential of 300 mV; S (3 cm^2) is the surface area; the number of 4 means 4 electrons transfer in OER; F is Faraday constant (96485.3 C mol^{-1}), and n is the metal ions molar number calculated from ICP results of the as-prepared catalysts.

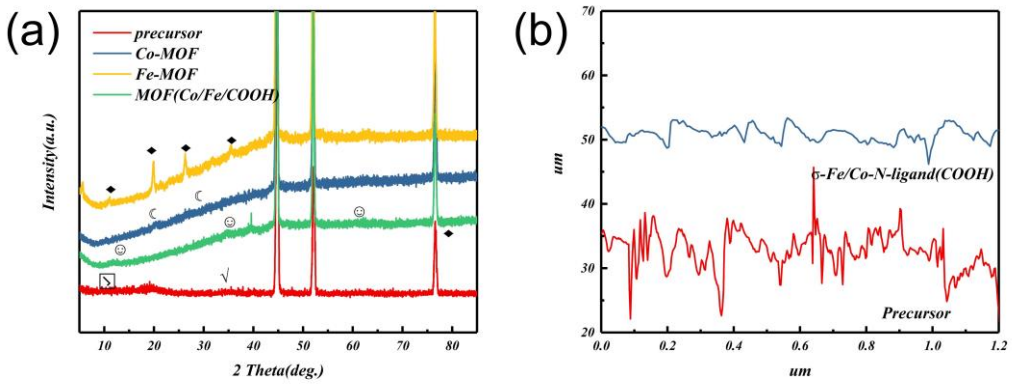

Figure S1 (a) XRD patterns of the Co-MOF, Fe-MOF and MOF(Co/Fe/COOH), (b) AFM image corresponding height profiles of σ-Fe/Co-N-ligand(COOH) and precursor.

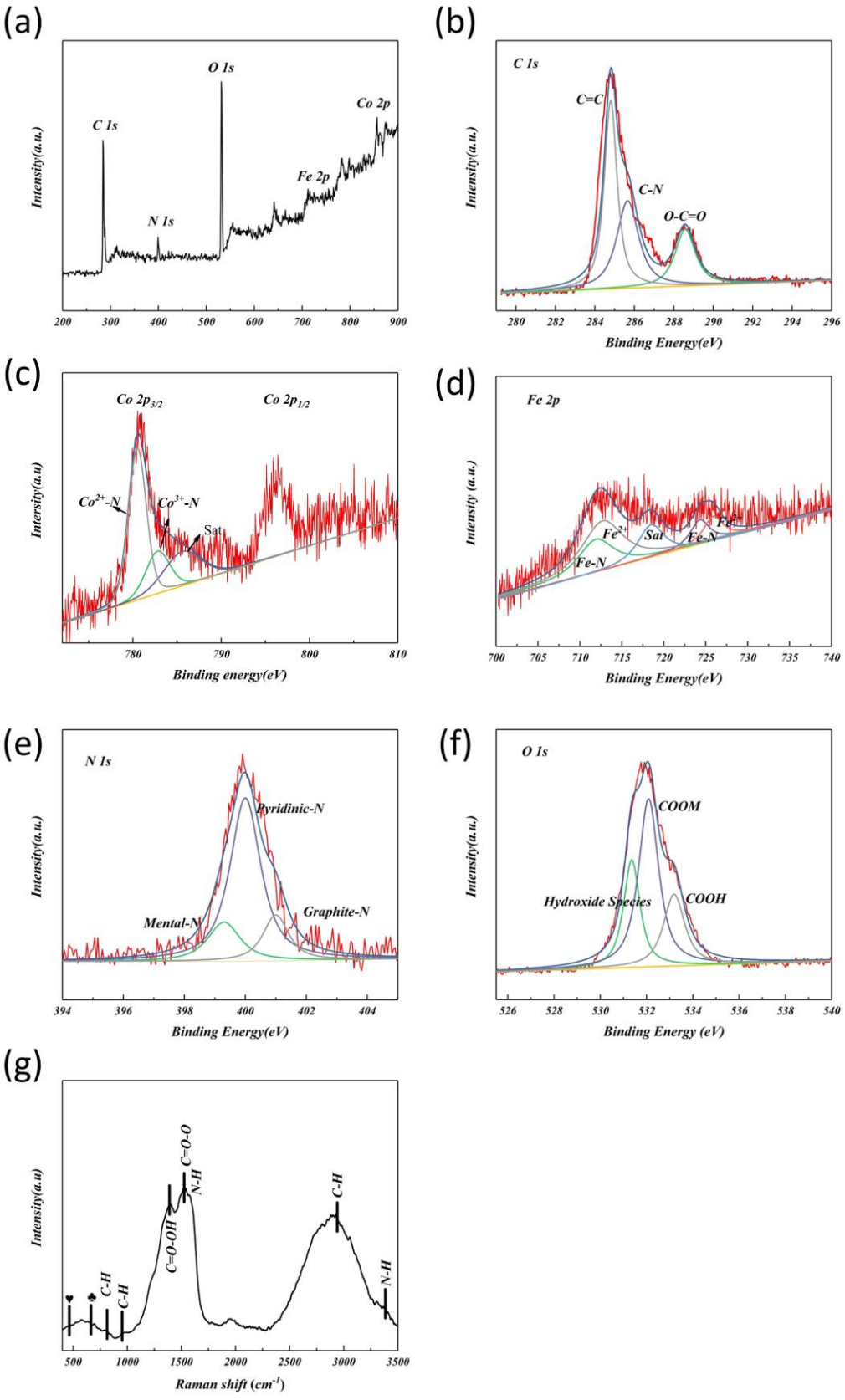
(a)
O 1s
Co 2p
C 1s
Fe 2p
N 1s
Intensity(a.u.)
200 300 400 500 600 700 800 900
(b)
C 1s
C=C
C-N
O-C=O
Intensity(a.u.)
280 282 284 286 288 290 292 294 296
Binding Energy(eV)
(c)
Co 2p3/2
Co 2p1/2
Co2+-N
Co3+-N
Sat.
Intersity(a.u)
780 790 800 810
Binding energy(eV)
(d)
Fe 2p
Fe2+
Sat
Fe-N
Fe3+
Intensity (a.u.)
700 705 710 715 720 725 730 735 740
Binding Energy(eV)
(e)
N 1s
Pyridinic-N
Mental-N
Graphite-N
Intensity(a.u.)
394 396 398 400 402 404
Binding Energy(eV)
(f)
O 1s
COOM
Hydroxide Species
COOH
Intensity(a.u.)
526 528 530 532 534 536 538 540
Binding Energy (eV)
(g)
C=O-O
N-H
C=O-OH
C-H
C-H
N-H
Intensity(a.u.)
500 1000 1500 2000 2500 3000 3500
Raman shift (cm-1)

Figure S2 XPS spectra of the σ-Fe/Co-N-ligand(COOH) catalyst. (a) Overall XPS spectrum, (b) C 1s, (c) Co 2p, (d) Fe 2p, (e) N 1s and (f) O 1s. (g) Raman spectra of σ-Fe/Co-N-ligand(COOH).

.

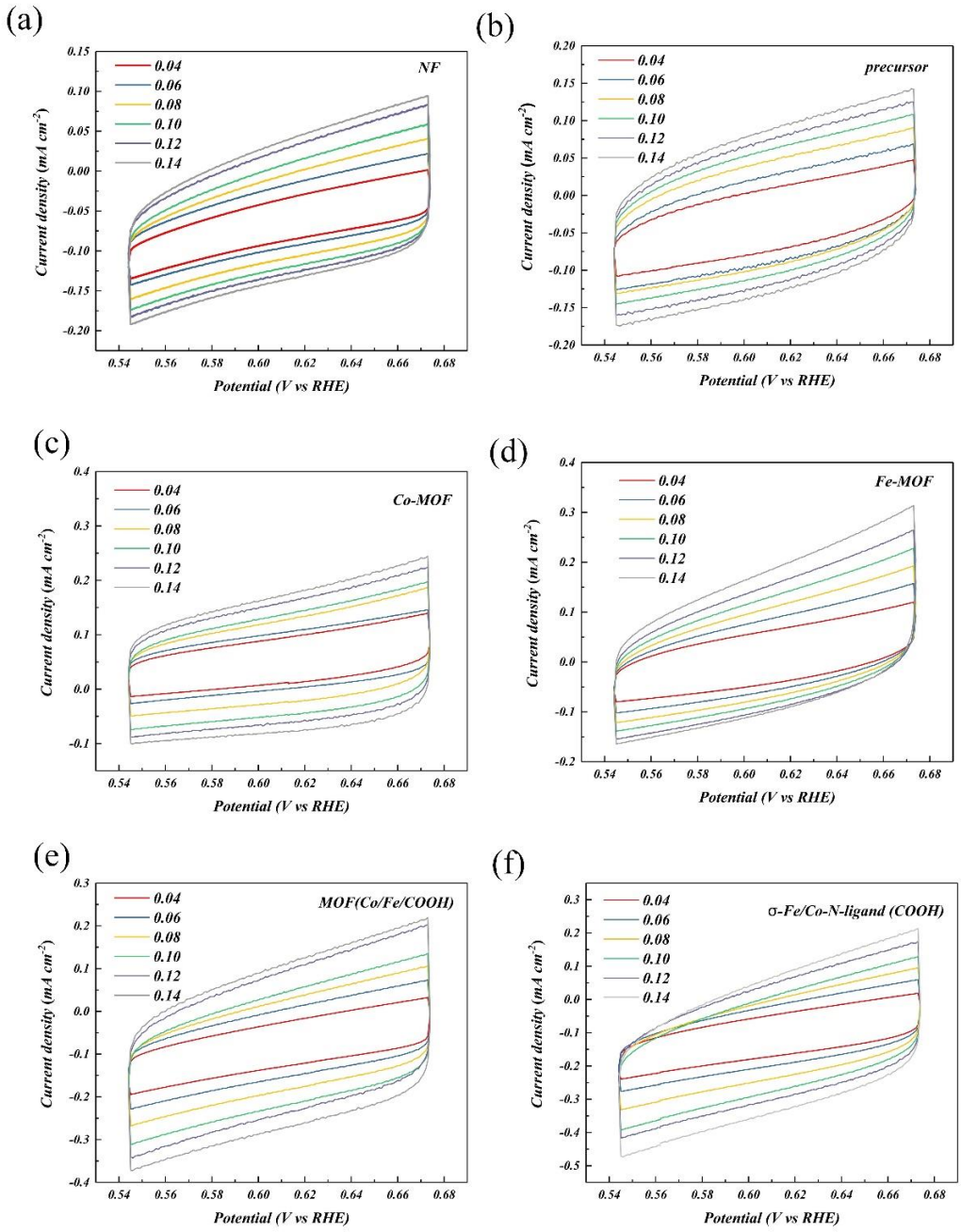

Figure S3 Capacitance study of the prepared of different samples. (a) NF, (b)

precursor, (c) Co-MOF, (d) Fe-MOF, (e) MOF(Co/Fe/COOH) and (f) σ-Co/Fe-N-ligand(COOH); the corresponding CVs measured at different scan rates from 40 to 140 mV s^{-1} current density at 0.609 V (vs. RHE) was plotted vs. scan rate.

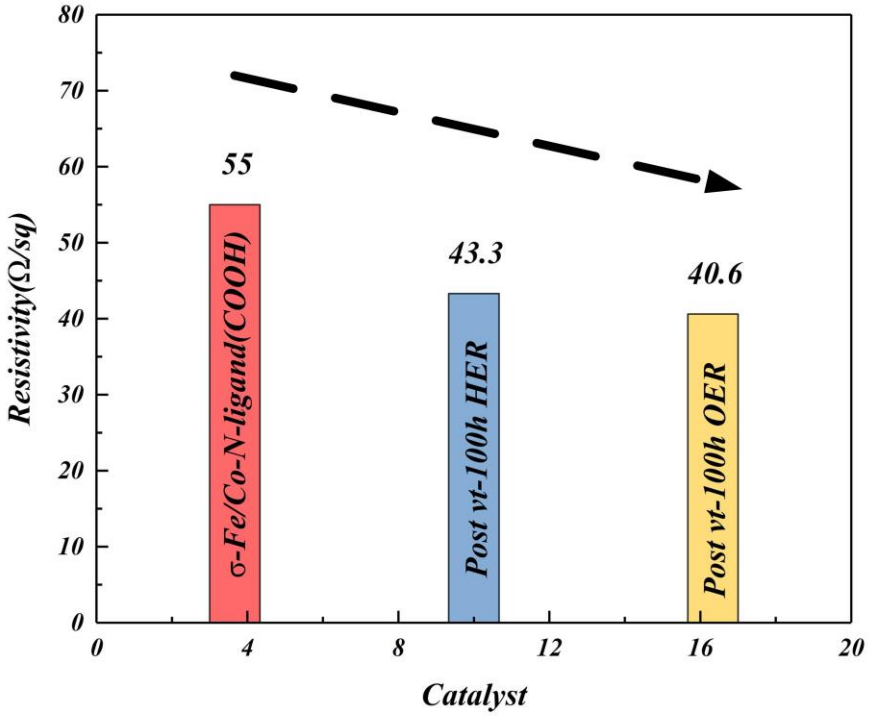

Figure S4 Averaged results of the four-point probe resistivity measurement of the assynthesized σ-Fe/Co-N-ligand(COOH) as well as the after vt-100 h catalytic experim

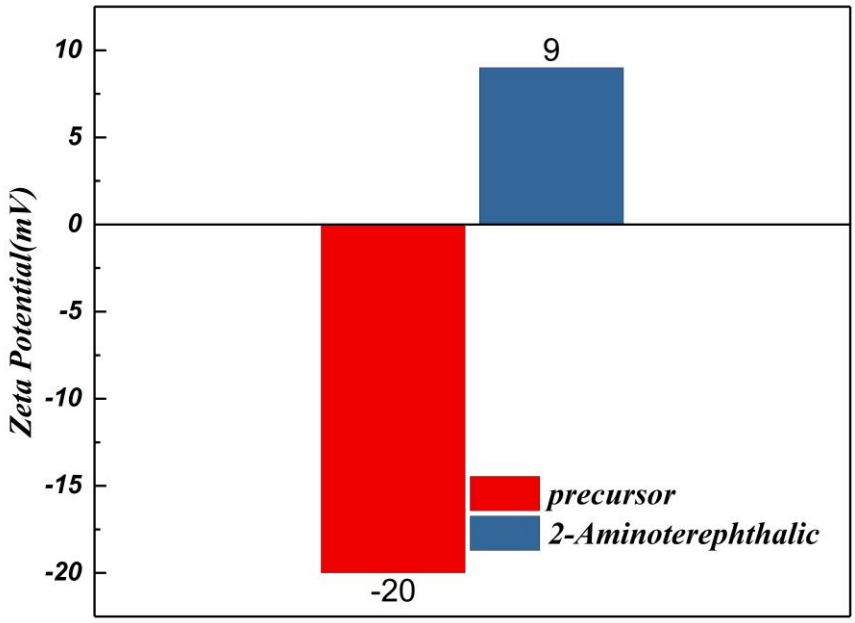

Figure S5 The zeta potential of precursor and 2-Aminoterephthalic Acid in water.

The testing dispersion was prepared by bath ultrasonication (1 h) of precursor (1 cm^2) and 2-Aminoterephthalic Acid (5 mg) in deionized water (2 mL), respectively.

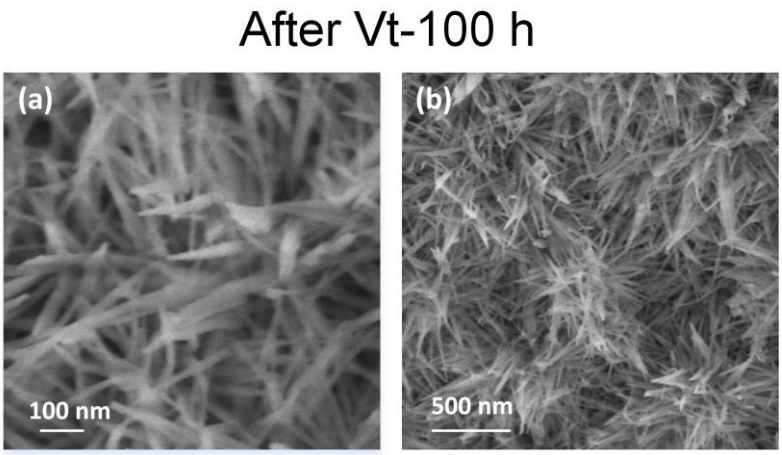

Figure S6 SEM patterns of after the 100 h V-t curve reation σ-Fe/Co-N-ligand(COOH).

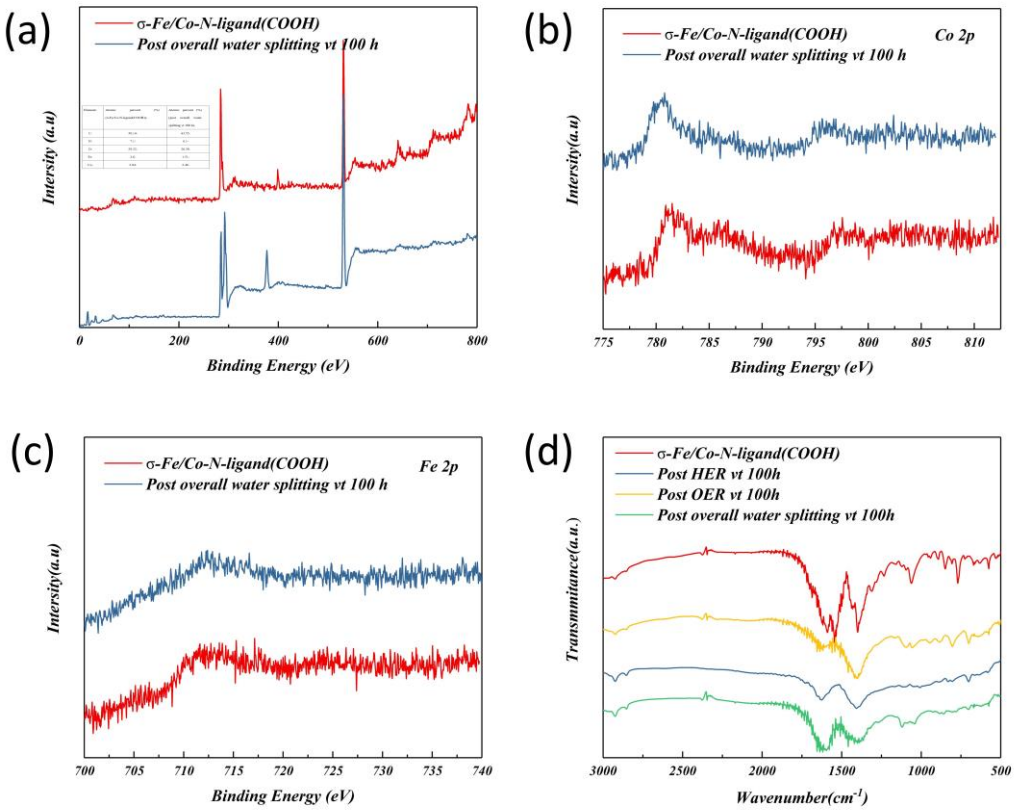

Figure S7 Stability study. (a-c) XPS patterns of after the 100 h V-t reation σ-Fe/Co-N-ligand(COOH). (d) FTIR spectra.

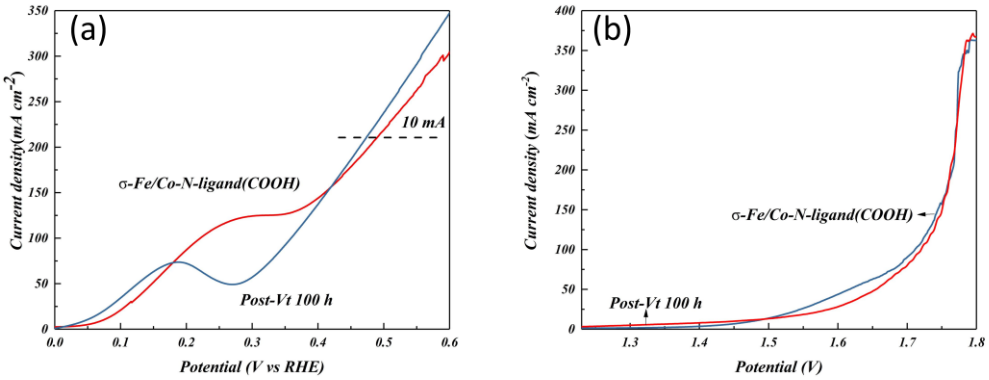

Figure S8 (a) OER LSV curves and (b) LSV curves of two-electrode cell at a scan rate of 5 mV/s.

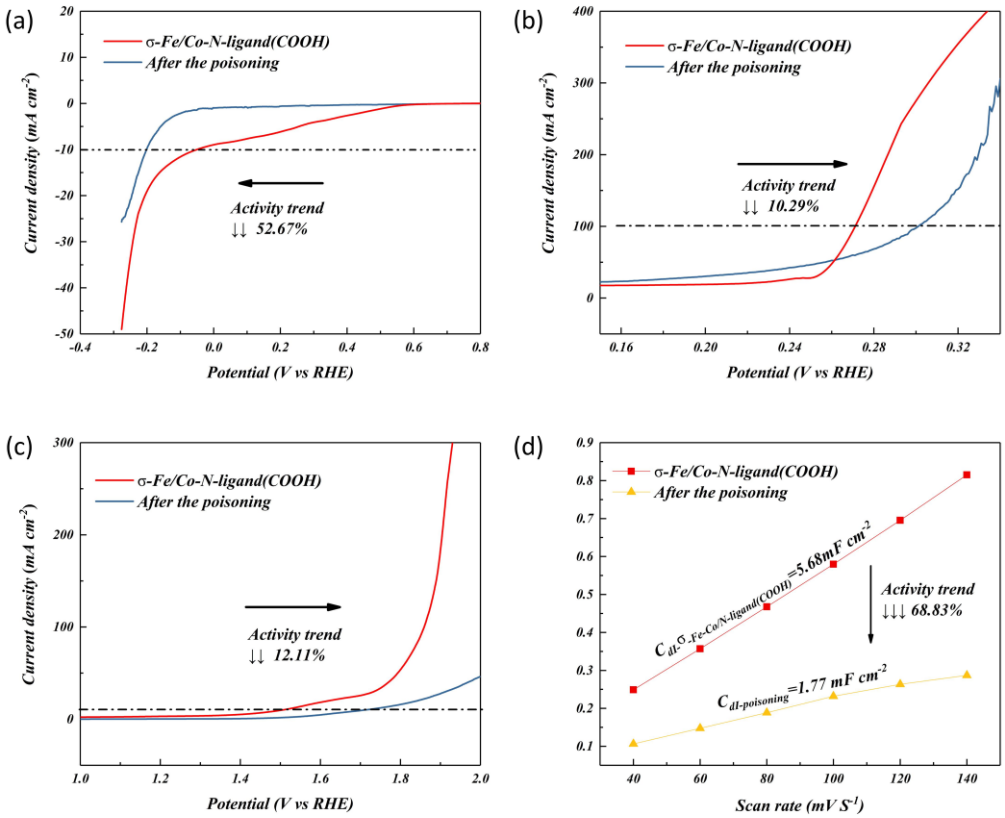

Figure S9 Metal toxicology study of σ-Co/Fe-N-ligand(COOH). (a) LSV profiles at 1 mV/s for HER. (b) LSV profiles at 1 mV/s for OER. (c) LSV profiles in two-electrode electrolyzer at 1 mV/s. (d) Estimation of double-layer capacitances (C_{dl}).

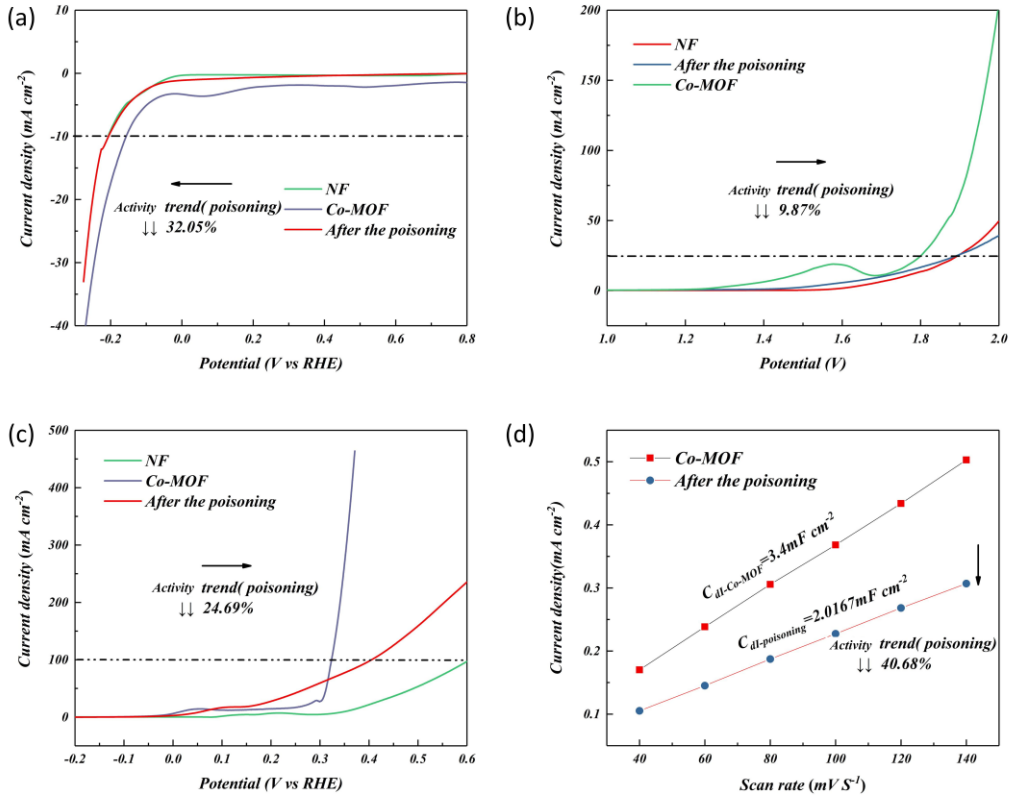

Figure S10 Metal toxicology study of Co-MOF. (a) LSV profiles at 1 mV/s for HER. (b) LSV profiles at 1 mV/s for OER. (c) LSV profiles in two-electrode electrolyzer in 1.0 M aqueous KOH solution at 1 mV/s. (d) Estimation of double-layer capacitances (C_{dl}).

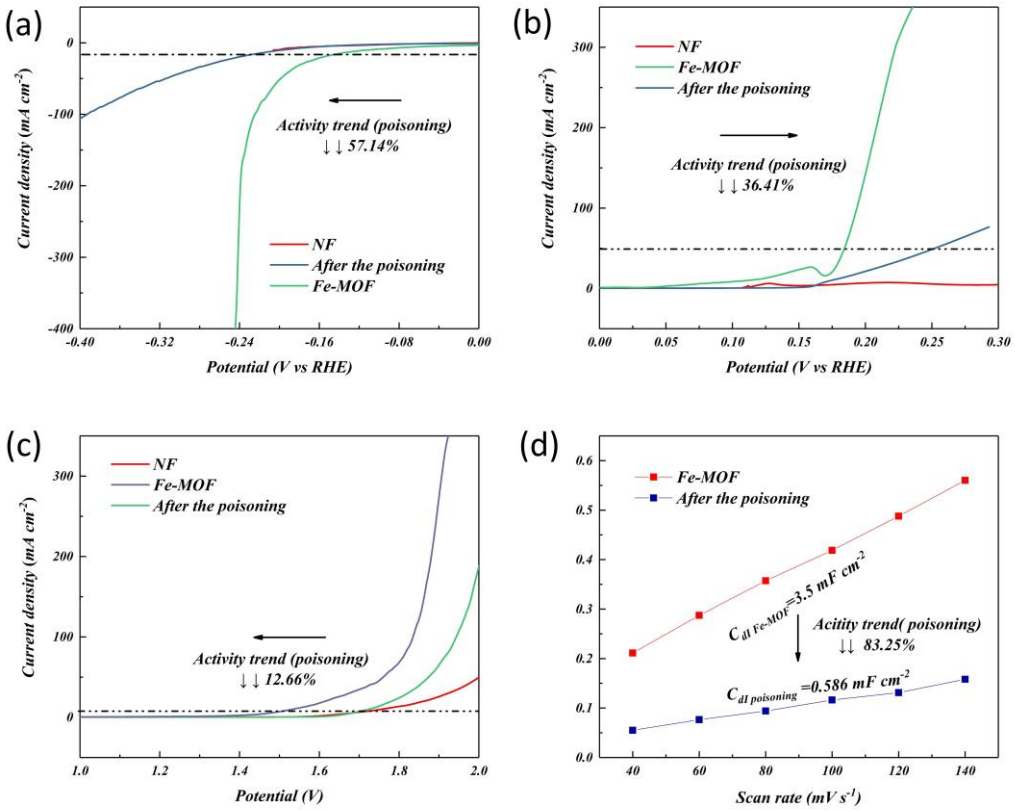

Figure S11 Metal toxicology study of Fe-MOF. (a) LSV profiles at 1 mV/s for HER. (b) LSV profiles at 1 mV/s for OER. (c) LSV profiles in two-electrode electrolyzer in 1.0 M aqueous KOH solution at 1 mV/s. (d) Estimation of double-layer capacitances (C_{dl}).

After SCN^- modification, the obvious HER performance is completely consistent with that of the NF. It was attributed to the poisoning of the metal and nitrogen centers. It should be noted that the overall water splitting performance is also close to that of commercial NF due to the sharp decrease in HER performance of the material and the decrease in OER performance. It is understandable that the overall water splitting performance of such material assembled as a bifunctional catalyst is not ideal.

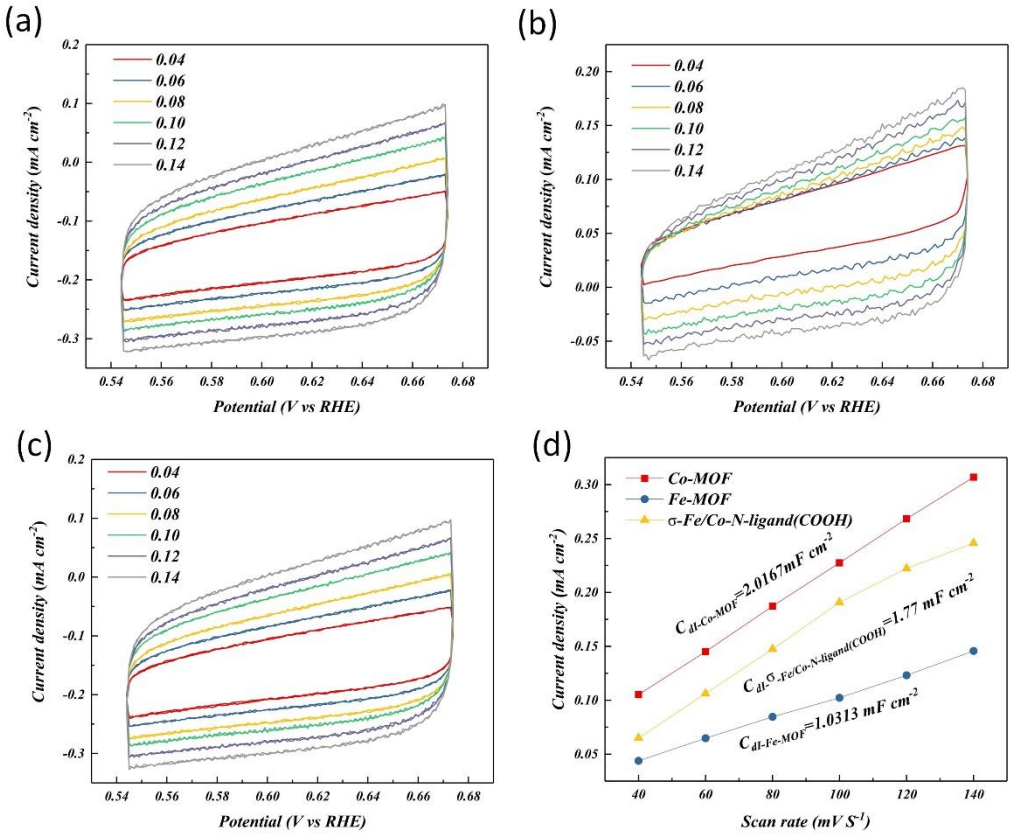

Figure S12 Capacitance study of the prepared of different samples. (a) Co-MOF after the poisoning, (b) Fe-MOF after the poisoning and (c) σ-Co/Fe-N-ligand(COOH) after the poisoning, the corresponding CVs measured at different scan rates from 40 to 140 mV s^{-1} current density at 0.609 V (vs. RHE) was plotted vs. scan rate. (d) Estimation of double-layer capacitances (C_{dl}) by plotting the current density variation ($\Delta j = (ja-jc)/2$), obtained from the (a)-(c) at 0.609 V vs RHE.

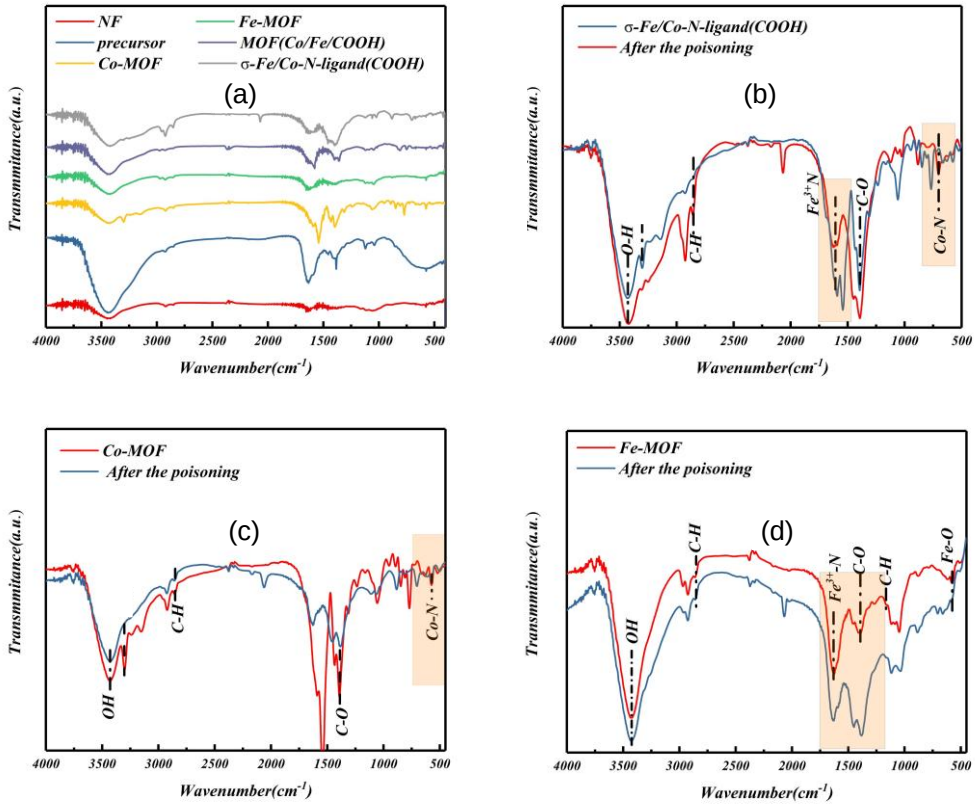

Figure S13 Metal toxicology study of σ-Co/Fe-N-ligand(COOH), Co-MOF and Fe-MOF. (a) The FTIR spectra of σ-Fe/Co-N-ligand(COOH), MOF(Co/Fe/COOH), Co-MOF, Fe-MOF, precursor, NF. Compare the MOF and after the poisoning (b-d) the FT-IR spectra of σ-Fe/Co-N-ligand(COOH), Co-MOF and Fe-MOF.

Table. S1. Summary of ICP results of σ-Fe/Co-N-ligand(COOH) and contrast material.

Samples	Co/Fe ratio in reactants	Metal content(Co+Fe) in MOF wt%
precursor	17:59	5.73%
Co-MOF	—	4.3%
Fe-MOF	—	1.85%
MOF(Co/Fe/COOH)	39:35	1.88%
σ-Fe/Co-N-ligand(COOH)	17:28	1.13%

Table. S2. EIS of σ-Fe/Co-N-ligand(COOH) and contrast material.

Samples	Rs(Ω)	Error	Error %	C(mF)	Error	Error %	Rct(Ω)	Error	Error %
NF	1.326	0.06588	4.9687	0.69885	3.241E-05	4.6512	261.1	3.179	6.537
Precursor	1.072	0.04841	4.5159	1.4041	7.8996E-05	5.6261	135.4	6.509	9.578
Co-MOF	0.9156	0.02828	3.0889	2.4136	9.3882E-05	3.897	125.6	4.781	9.73
Fe-MOF	1.238	0.03838	3.1007	6.601	0.00031521	4.4328	28.99	3.853	3.291
MOF(Co/Fe/COOH)	1.006	0.03516	3.4954	1.9152	8.7476E-05	4.5675	106.1	7.6	6.588
σ-Fe/Co-N-ligand(COOH)	0.9808	0.02808	2.8619	2.5524	0.00010063	3.9426	90	3.942	9.573

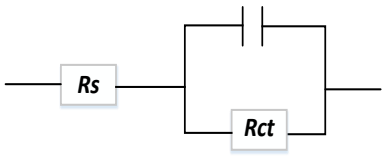

Table. S3. Comparison of performance of MOF and MOF derivatives as bifunctional electrocatalysts for overall water splitting in alkaline environments.

Samples	Electrolytes (HER)	HER η_a (mV)	OER η_b (mV)	Overall water splitting cell voltage[c] (V)	Overall water splitting work life(h)	Ref
σ-Fe/Co-N-ligand (COOH)	1M KOH	128	60	1.468	100	This work
CuRu-MOF	0.5 M H_2SO_4	61.6	31	1.53	24	[1]
NH_2-MIL 88B(Fe_2Ni)-(MOF)	1M KOH	87	240	1.56	30	[2]
Co/CoN/Co_2P-NPC	1M KOH	99	272	1.60	48	[3]
Co_3S_4/EC-MOF	1M KOH	84	226	1.55	12	[4]
Mo-CoP	1M KOH	96	305	1.56	20	[5]
Fe-Ni@NC-CNTs	1M KOH	274	202	1.98 at 145 mA cm^{-2}	40000s	[6]
NF@Ni/C-600	1M KOH	33	265	1.60 at 35.9 mA cm^{-2}	70	[7]
CoPO	1M KOH	158	280	1.52	10	[8]
Co/NBC	1M KOH	117	302	1.68	40000s	[9]
NiCoSe/C	1M KOH	143	249	1.68	20	[10]

Reference

1. T. Qiu, Z. Liang, W. Guo, S. Gao, C. Qu, H. Tabassum, H. Zhang, B. Zhu, R. Zou and Y. Shao-Horn, *Nano Energy*, 2019, **58**, 1-10.
2. D. Senthil Raja, X.-F. Chuah and S.-Y. Lu, *Adv. Energy Mater.*, 2018, **8**.
3. L. Hu, Y. Hu, R. Liu, Y. Mao, M. S. Balogun and Y. Tong, *Int. J.Hydrog. Energy*, 2019, **44**, 11402-11410.
4. T. Liu, P. Li, N. Yao, T. Kong, G. Cheng, S. Chen and W. Luo, *Adv. Mater.*, 2019, **31**, e1806672.
5. C. Guan, W. Xiao, H. Wu, X. Liu, W. Zang, H. Zhang, J. Ding, Y. P. Feng, S. J. Pennycook and J. Wang, *Nano Energy*, 2018, **48**, 73-80.
6. X. Zhao, P. Pachfule, S. Li, J. R. J. Simke, J. Schmidt and A. Thomas, *Angew. Chem. Int. Ed .Engl.*, 2018, **57**, 8921-8926.
7. H. Sun, Y. Lian, C. Yang, L. Xiong, P. Qi, Q. Mu, X. Zhao, J. Guo, Z. Deng and Y. Peng, *Energ. Environ. Sci.*, 2018, **11**, 2363-2371.
8. G. Anandhababu, Y. Huang, D. D. Babu, M. Wu and Y. Wang, *Adv. Funct. Mater.*, 2018, **28**.
9. M.-R. Liu, Q.-L. Hong, Q.-H. Li, Y. Du, H.-X. Zhang, S. Chen, T. Zhou and J. Zhang, *Adv. Funct. Mater.*, 2018, **28**.
10. Z. Chen, B. Xu, X. Yang, H. Zhang and C. Li, *Int. J.Hydrog. Energy*, 2019, **44**, 5983-5989.